TRAJECTORY GENERATION FOR SPATIAL HUMANOID ROBOTS USING ASSUR'S VIRTUAL CHAINS THROUGH SCREW THEORY

Gustavo S. Toscano, gustavo.toscano@posgrad.ufsc.br
Universidade Federal de Santa Catarina, Centro Tecnológico, Departamento de Automação e Sistemas, Florianópolis/SC, CEP 88040-900, P.O. Box 476, Brasil.
Henrique Simas, simas@emc.ufsc.br
Universidade Federal de Santa Catarina, Centro Tecnológico, Departamento de Engenharia Mecânica, Florianópolis/SC, CEP 88040-900, P.O. Box 476, Brasil.
Eugênio B. Castelan, eugenio.castelan@ufsc.br
Universidade Federal de Santa Catarina, Centro Tecnológico, Departamento de Automação e Sistemas, Florianópolis/SC, CEP 88040-900, P.O. Box 476, Brasil.

Abstract: *This paper presents the kinematic model and a strategy of trajectory generation for a spatial humanoid robots (HRs) using the concept of floating base through the screw theory and its tools: Assur's virtual chains and Davies's method. The resulting mechanism is a complex spatial parallel mechanism with four loops. Associating Davies's method, the differential kinematics of the spatial HR was modeled and the Jacobian matrix was obtained. Thus, the velocities of the "real" joints were obtained by using the inverse of that Jacobian and their position were obtained by means of numerical methods. The kinematic model and the trajectory generation were developed including the ZMP as a gait stability criterion. The used modeling approach allowed to obtain a single kinematic representation of a biped robot motion which is independent from any fixed reference frame, and also independent of the degree of freedom of robotic mechanisms. The modeling approach was applied to a specific HR (Bioloid, from Robotis) and the trajectory generation was developed using the geometric constraints method by the Assur's virtual chains. The related results are presented graphically from computer simulations.*

Keywords: *Trajectory Generation, Humanoid Robots, Floating Base, Davies's Method.*

1. INTRODUCTION

Humanoids robots (HR's) are a great deal because this kind of robot can manipulate objets and also because the biped motion is one of a few that can access almost every kind of terrains (Westervelt *et al.*, 2007). Thus, it is of great importance the continuing studies about the modeling and the trajectory generation for biped and HR's.

About the kinematic modeling, there are two methods commonly used to model the kinematics of robots: the first based on the Denavit-Hartenberg (DH) convention (Denavit, 1955) and another based on screw theory (ST) (Hunt, 2000; Davidson and Hunt, 2004). While the DH method is largely used in literature (Rocha *et al.*, 2011), the ST approach is less known.

Rocha *et al.* (2011) pointed out some advantages of the ST over DH convention. The flexibility of reference choices in the successive screw displacements method is a remarkable feature, since it is not complex the process of identification of the parameters and it can be used to obtain simplified equations. Screw-based modeling presents its main advantages in differential kinematics models in which the respective Jacobian is formed by the normalized screws of the kinematic chain (Rocha *et al.*, 2011).

The inverse differential kinematics can be solved by inverting the Jacobian or by using the Davies's method and virtual chains to define the end-effector's movement (Campos *et al.*, 2005). Besides the advantages of the ST for robot kinematic modeling, the majority of works in the fields of humanoid robotics still uses DH parameters.

Gal *et al.* (2004) applied ST to analyse the human mandibular mechanics. In (Sabater *et al.*, 2006), the ST was used to design and to analyse a spherical humanoid neck. Zhu *et al.* (2009) used ST to model the kinematics of a Steward platform and made an analogy that his approach may be a novel parallel robot for rotary humanoid wrist.

Man *et al.* (2007) presented a work making a kinematic analysis of an humanoid structure by the ST. Besides showing how to use the ST to solve the direct and inverse kinematics of an HR and indicating the use of the screw-based Jacobian to solve its differential kinematics, there is a lack of clarity that would clarify the comprehension of the use of the ST in HB's.

In Sánchez *et al.* (2011), the ST was used to solve the inverse kinematic of the AH1N1 HR. Despite of solve the inverse kinematic using ST, the authors solved the direct kinematic by the DH convention and nothing was said about the differential kinematic of the humanoid.

About trajectory generation to humanoid and biped robots, basically, there are some manners (used in the literature) to generate humanoid trajectories: by the 3D inverted pendulum approach (3D-LIP) (Kajita *et al.*, 2001); by capturing in video the human motion (Hoonsuwan *et al.*, 2009) and adapting it to be executed by the robot; by the geometric constraint

method (Huang *et al.*, 2001; Wang *et al.*, 2009); by kinematic motion primitives (KMPs) (Moro *et al.*, 2011, 2012) which are used for reconstruction of the center of mass motion; and a mix between the KMPs and 3D-LIP approaches (Hugel and Jouandeau, 2012).

In works of (Mu and Wu, 2004; Wang *et al.*, 2009; Hoonsuwan *et al.*, 2009; Moro *et al.*, 2011, 2012), a biped robot was modeled using the DH parameters. Thus, they elaborated their trajectories by considering two kinematics representations for the same mechanic structure. That is, the gait would be performed by switching between two models depending on which foot is supporting the robot (Toscano *et al.*, 2011); even the 3D-LIP approach needs a switching structure, because one biped robot corresponds to two 3D-LIP's.

However, Sentis (2007) and Mistry *et al.* (2008) applied the floating base (FB) concept by recognizing that a biped robot can walk freely above a terrain in a similar way that a spacecraft is free to travel through space. By the use of the FB concept, the biped structure can be represented by just one kinematic model detached from an inertial reference frame and the switching between kinematic models is not necessary to perform a gait.

This work aims to present, in a systematic way, how a full body HR can be modeled using ST and its tools. Further, the virtual chains are used to impose motion to the real chains. Hence, it was chosen the geometric constraint method (Huang *et al.*, 2001; Wang *et al.*, 2009) to generate a gait because, besides being intuitive, to apply this method, it is not necessary to use the switching models structure. Lastly, the ZMP criterion, as in (Kajita *et al.*, 2001), is used to test whether the generated trajectory is feasible and/or does not make the HR fall down on the ground.

This paper is organized as follows: first, the ST and its tools are briefly presented. Then, it is shown how may model the kinematics of an HR by using virtual chains and the Davies's method. After that, the trajectory generated is presented and, then, the simulation results are shown.

2. SCREW-BASED KINEMATIC TOOLS

This paper is based on the method of successive screw displacement, on the screw representation of differential kinematics, on the Davies's method and on the Assur's virtual chain concept. These tools and their application are discussed and exemplified in several papers (Tsai, 1999; Hunt, 2000; Campos *et al.*, 2005; Santos *et al.*, 2006; Guenther *et al.*, 2008). In order to simplify the comprehension and the development of the HB model, some of these fundamentals are briefly presented in this section.

2.1 Successive Screw Displacements Method

Charle's theorem states that the general spatial displacement of a rigid body is a rotation about an axis and a translation along the same axis. Such combination of translation and rotation is called a screw displacement (Bottema and Roth, 1979).

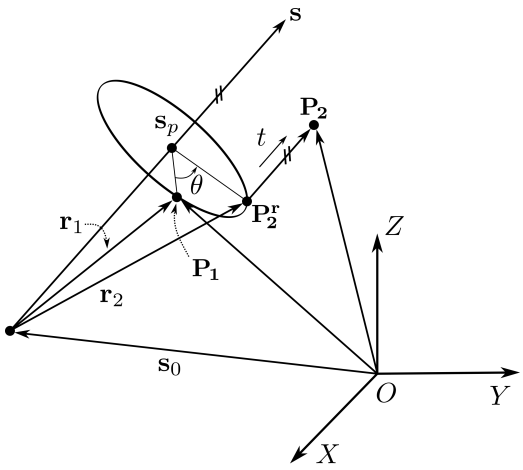

Figure 1: Vector diagram of a spatial displacement.

In Fig. 1, it can be seen a point $\mathbf{P}$ of a rigid body displaced from the first position $\mathbf{P_1}$ to the second position $\mathbf{P_2}$ by a rotation of θ, about a screw axis, followed by a translation of t along the same axis. The rotation brings $\mathbf{P}$ from $\mathbf{P_1}$ to $\mathbf{P_2^r}$, and the translation brings $\mathbf{P}$ from $\mathbf{P_2^r}$ to $\mathbf{P_2}$. On Fig. 1, $\mathbf{s} = \begin{bmatrix} s_x & s_y & s_z \end{bmatrix}^T$ denotes a unit vector along the direction of the screw axis, and $\mathbf{s_0} = \begin{bmatrix} s_{0_x} & s_{0_y} & s_{0_z} \end{bmatrix}^T$ denotes the position vector of a point lying on the screw axis. These screw parameters together with the screw axis completely define the general displacement of a point attached to a rigid body and define a general displacement of a rigid body (Tsai, 1999; Ribeiro and Martins, 2010).

Representing the first position $\mathbf{P_1}$ as the vector $\mathbf{p_1} = \begin{bmatrix} p_{1_x} & p_{1_y} & p_{1_z} \end{bmatrix}^T$ and the second $\mathbf{p_2} = \begin{bmatrix} p_{2_x} & p_{2_y} & p_{2_z} \end{bmatrix}^T$, the general screw displacement for a rigid body can be given by the Rodrigues's formula as

$$\mathbf{p_2} = \mathbf{R}(\theta)\,\mathbf{p_1} + \mathbf{d}(t), \tag{1}$$

where $\mathbf{R}(\theta)$ is the rotation matrix corresponding to the rotation θ about the screw axis and $\mathbf{d}(t)$ is the displacement vector corresponding to the translation of t along the screw axis.

Considering the augmented vectors $\hat{\mathbf{p}}_\mathbf{1} = \begin{bmatrix} \mathbf{p_1}^T & 1 \end{bmatrix}^T$ and the second $\mathbf{P_2}$ as $\hat{\mathbf{p}}_\mathbf{2} = \begin{bmatrix} \mathbf{p_2}^T & 1 \end{bmatrix}^T$, the general displacement of a rigid body - Eq. (1) - can be represented by a homogeneous transformation given by ((Tsai, 1999) for more details):

$$\hat{\mathbf{p}}_\mathbf{2} = \mathbf{A}(\theta, t)\,\hat{\mathbf{p}}_\mathbf{1}. \tag{2}$$

2.1.1 Successive Screw Displacements

The screw representation of the homogeneous transformation will be use here to express the composition of two or more screw displacements applied successively to a rigid body.

A kinematic chain is composed by rotational and prismatic joints numbered from 1 to n. Each joint describes the displacement between two successive links starting from the base frame, defined as the *Link* 0, untill the last link of the kinematic chain, defined as *Link n*. Thus, the joint i describes the relative displacement between the links i and $i-1$. The position and the orientation of a point on a *Link k* with respect to a *Link c* of the same considered chain can be defined as (Simas, 2008):

$$\mathbf{A_k^c} = \bar{\mathbf{A}}_\mathbf{r}^\mathbf{c} \left(\prod_{i=c+1}^{k} \mathbf{A_{q_i}^r} \right) \bar{\mathbf{A}}_\mathbf{k}^\mathbf{r}, \tag{3}$$

where r indicates the link in which a coordinate system is fixed; $\mathbf{A_k^c}$ is the homogeneous matrix that describes the position and orientation of a point on the *Link k* with respect to a coordinate system attached on the *Link c*; $\bar{\mathbf{A}}_\mathbf{r}^\mathbf{c}$ is the homogeneous matrix defined in the initial position of the chain that describes the position and orientation of the reference coordinate system attached on *Link r* with respect to the coordinate system on *Link c*; $\bar{\mathbf{A}}_\mathbf{k}^\mathbf{r}$ is the homogeneous matrix also defined in the initial position of the chain that describes the position and orientation of the coordinate system of a point on *Link k* with respect to the reference on *Link r*; and $\mathbf{A_{q_i}^r}$ is the homogeneous matrix that describes the relative displacement between the links i and $i-1$ described by the screws defined with respect to the reference coordinate system attached on *Link r*.

2.2 Screw Representation of Differential Kinematics

The complete displacement of the rigid body by means of a rotation and a translation with respect to the same axis is called screw movement (or twist): \$. The ration of the linear and angular velocities is called pitch of the screw: $h = \frac{\|\tau\|}{\|\omega\|}$.

The twist \$ is composed by a pair of vectors as $\$ = \begin{bmatrix} \omega^T & \mathbf{v_p}^T \end{bmatrix}^T$, in which ω represents the angular velocity with respect to the inertial frame and $\mathbf{v_p}$ represents the linear velocity of a point $\mathbf{P}$ attached to the body which is instantaneously coincident with the origin $\mathbf{O}$ of the reference frame (Tsai, 1999). A twist may be decomposed into its magnitude and its corresponding normalized screw (Davidson and Hunt, 2004). In this paper, the twist magnitude, denoted as $\dot{q}$, is either the magnitude of the angular velocity $\|\omega\|$ of the body if the joint is rotative, or its linear velocity $\|\mathbf{v_p}\|$ if the joint is prismatic.

The twist \$ is completely defined by the vectors $\mathbf{s}$ and $\mathbf{s_0}$, and the scalar pitch. It can be decomposed into a normalized screw $\hat{\$}$ and a magnitude $\dot{q}$ as

$$\$ = \begin{bmatrix} \omega \\ \mathbf{v_p} \end{bmatrix} = \begin{bmatrix} \omega \\ \mathbf{s_0} \times \omega + h\omega \end{bmatrix} = \begin{bmatrix} \mathbf{s} \\ \mathbf{s_0} \times \mathbf{s} + h\mathbf{s} \end{bmatrix} \dot{q} = \hat{\$}\dot{q}. \tag{4}$$

In a kinematic chain, the relative velocity state between two link is obtained by the sum of the twists of the kinematic pairs between them (Rocha *et al.*, 2011). For instance, in a robot, the angular and linear velocities of its end-effector, $\$_\mathbf{ef}$, with respect to the base b of the robot may be expressed as:

$$\$_\mathbf{ef} = \begin{bmatrix} \omega_\mathbf{ef} \\ \mathbf{v}_{\mathbf{p}_\mathbf{ef}} \end{bmatrix} = \sum_{i=b+1}^{ef} \hat{\$}_\mathbf{i}\dot{\mathbf{q}}_\mathbf{i} \;\Rightarrow\; \$_\mathbf{ef} = \mathbf{J}\dot{\mathbf{q}}_\mathbf{i}, \tag{5}$$

where $\hat{\$}_\mathbf{i}\dot{\mathbf{q}}_\mathbf{i}$ express the velocity between the link i with respect to link $i-1$. The normalized screws column vectors compose the screw Jacobian matrix $\mathbf{J}$ and the column vector $\dot{\mathbf{q}} = \begin{bmatrix} \dot{q}_1 & \dots & \dot{q}_{ef} \end{bmatrix}^T$ is formed by the magnitudes of the screws (Hunt, 2000).

The sum in Eq. (5) is possible if all twists are defined according to the same referential coordinate frame. However, there are situations in which some twists are defined in differents referentials, in these cases, a screw transformation $\mathbf{T_j^i}$, as presented in Eq. (6),

$$\mathbf{T_j^i} = \begin{bmatrix} \mathbf{R_j^i} & \mathbf{0} \\ \widehat{\mathbf{p}}_\mathbf{j}^\mathbf{i}\mathbf{R_j^i} & \mathbf{R_j^i} \end{bmatrix}, \tag{6}$$

must be applied to these twists to express them in the desired referential (Tsai, 1999). This information is also useful when the kinematic analysis must consider different reference points in the workspace. The $\mathbf{T_j^i}$ matrix indicates that the transformation occurs from the referential j to the referential i, $\widehat{\mathbf{p}}_\mathbf{j}^\mathbf{i}$ is the skew-symmetric matrix composed by the elements of the position vector $\mathbf{p_j^i}$, and $\mathbf{R_j^i}$ express the orientation of the frame j with respect to the frame i.

2.3 Assur's Virtual Chains

A kinematic chain can be used to define or to monitor the displacement of a single body, which is useful for motion analysis of serials chains in multirobot systems (cooperative robotics). Thus, a virtual kinematic chain representing motion in a coordinate system is adopted. The use of virtual chains for this objective was proposed in Santos *et al.* (2006) based

on the work of Campos *et al.* (2005) who further developed the concept of Assur's virtual chains. Virtual chains can also be linked to real chains to monitor or to impose motion to a particular link of the real chain (see Campos *et al.* (2005); Santos *et al.* (2006) for more details).

Considering the Assur's virtual chain 3P3R attached in a serial chain of n joints. The linear velocity of the real link n that is instantaneously coincident with the origin of the reference frame. Thus, the resulting movement of the real link $n+1$ with respect to link 0 is obtained adding linearly the joints normilized twists of the virtual chain given by (Tsai, 1999):

$$\dot{\mathbf{x}} = \begin{bmatrix} \boldsymbol{\omega} \\ \mathbf{v_O} \end{bmatrix} = \begin{bmatrix} \hat{\$}_{\mathbf{px}} & \hat{\$}_{\mathbf{py}} & \hat{\$}_{\mathbf{pz}} & \hat{\$}_{\mathbf{rx}} & \hat{\$}_{\mathbf{ry}} & \hat{\$}_{\mathbf{rz}} \end{bmatrix} \begin{bmatrix} \dot{q}_{px} & \dot{q}_{py} & \dot{q}_{py} & \dot{q}_{rx} & \dot{q}_{ry} & \dot{q}_{rz} \end{bmatrix}^T, \tag{7}$$

in which the matrix formed by the normalized screws is the screw Jacobian matrix. As this Jacobian is an 6×6 matrix, then, it can be inverted to solve the inverse differential kinematics of the 3P3R virtual chain.

2.4 Davies's Method

Davies's method is a systematic manner to solve the differential kinematics of closed chain mechanisms. Davies (1981) derives his method from the Kirchhoff's circulation law for electrical circuits. The Kirchhoff-Davies law states that "the algebraic sum of relative velocities of kinematic pairs along any closed mechanism is zero" (Davies, 1981). Considering a closed chain composed by n joints, and that the velocity of one of its link with respect to itself is null (Campos *et al.*, 2005; Santos *et al.*, 2006), then, the circulation law may be expressed as:

$$\sum_{i=1}^{n} \hat{\$}_{\mathbf{i}} \dot{q}_i = \mathbf{0}, \tag{8}$$

in which $\hat{\$}_{\mathbf{i}}$ is the normalized twist, $\dot{q}_i$ is the magnitude of $\$_{\mathbf{i}}$ and $\mathbf{0}$ is a vector whose dimension is equal to the dimension of $\hat{\$}_{\mathbf{i}}$. Equation (8) is the constraint equation and it can be generalize as:

$$\mathbf{N}\dot{\mathbf{q}} = \mathbf{0}, \tag{9}$$

where $\mathbf{N} = \begin{bmatrix} \hat{\$}_{\mathbf{1}} & \hat{\$}_{\mathbf{2}} & \dots & \hat{\$}_{\mathbf{n}} \end{bmatrix}$ is the network matrix containing the normalized screws whose signals depend on the screw definition in the circulation law orientation, and $\dot{\mathbf{q}} = \begin{bmatrix} \dot{q}_1 & \dot{q}_2 & \dots & \dot{q}_n \end{bmatrix}^T$ is the magnitude vector.

The Kirchhoff-Davies circulation law may be applied to mechanisms that contain n circuit. In this case, considering that a mechanism is composed by k circuits, thus, the network matrix in Eq. (9) would have k rows of screws, each one corresponding to a closed circuit.

In a closed kinematic chain, ones may identify primary and secondary joints to handle actuated and passive joints, respectively. Using the constraint equation Eq. (9), the secondary joint velocities can be calculated as function of the primary joint velocities (Davies, 1981; Campos *et al.*, 2005; Santos *et al.*, 2006). To this end, the same equation earlier cited is rearranged in a manner to highlight the primary and secondary joint velocities as:

$$\begin{bmatrix} \mathbf{N_s} & \mathbf{N_p} \end{bmatrix} \begin{bmatrix} \dot{\mathbf{q}}_\mathbf{s} \\ \dot{\mathbf{q}}_\mathbf{p} \end{bmatrix} = \mathbf{0}, \tag{10}$$

where $\mathbf{N_p}$ and $\mathbf{N_s}$ are the primary and secondary network matrices, respectively, and $\dot{\mathbf{q}}_\mathbf{p}$ and $\dot{\mathbf{q}}_\mathbf{s}$ are the corresponding primary and secondary magnitude vectors, respectively. Thus, if the $\mathbf{N_s}$ network matrix is square and invertible, the secondary joint velocities may be determined as:

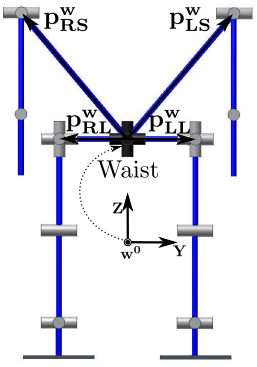

Figure 2: 3D Model of an humanoid structure.

$$\dot{\mathbf{q}}_\mathbf{s} = -\mathbf{N}_\mathbf{s}^{-1}\mathbf{N}_\mathbf{p}\dot{\mathbf{q}}_\mathbf{p}. \tag{11}$$

3. KINEMATIC MODELING OF AN HUMANOID ROBOT USING SCREW THEORY

In the previous section, it was briefly presented the basis of ST and its tools that will be used in the current section to model the HR Bioloid, from Robotis.

3.1 Bioloid Humanoid Robot

Bioloid is an HR composed by one FB (see Papadopoulos and Dubowsky (1991), Sentis (2007) and Mistry *et al.* (2008) for more details) link and four serial chains that mimic the four limbs of the human body. It has $1,7$ Kg, with

$0,397$ *m* of high and its structure is composed by eighteen actuated joints: three degree of fredom (DoF) for each arm and six DoF for each leg.

A 3D CAD model of an humanoid structure is depicted in Fig. 2. In the same figure, the waist of the humanoid chain is identified as its FB which is free to move through space. The waist is the local reference on the humanoid kinematic chain, that is, the position of the arms and the legs are given with respect to it.

The mass and length of the links of the humanoid structure are given in the Tab. 1. The position of the shoulders and the thigh, with respect to the waist, are given in Tab. 2. For the sake of simplicity, the position of the center of mass of the links is right in the middle of each associated link. However, the position of the center of mass of the trunk, with respect to the waist, is given by the position vector $\mathbf{p}^{\mathbf{w}}_{\mathbf{T_{CM}}} = \begin{bmatrix}-0,014563 & 0 & 0,086397\end{bmatrix}^T$.

Table 1: Mass and length of the components of the HR.

Components	**Mass** (Kg)	**Length** (m)
Torso	$0,6748$	–
Upper-arm	$0,06664$	$0,06931$
Forearm	$0,06215$	$0,05178$
Thigh	$0,15586$	$0,0773829$
Calf	$0,19589$	$0,0780929$
Foot	$0,03206$	$0,030779$

Table 2: Position of the shoulders and the thighs with respect to the waist.

Components	**Vectors** (m)
Right shoulder	$\begin{bmatrix}0 & -0,064646 & 0,121451\end{bmatrix}^T$
Left shoulder	$\begin{bmatrix}0 & 0,064646 & 0,121451\end{bmatrix}^T$
Right thigh	$\begin{bmatrix}0 & -0,042165 & 0\end{bmatrix}^T$
Left thigh	$\begin{bmatrix}0 & 0,042165 & 0\end{bmatrix}^T$

3.2 Modeling of The Bioloid Robot Using Screw Theory

In this section, the kinematic modeling of the Bioloid robot by the ST and its tools will be presented. Because of the bilateral symmetry of the HR structure and because it is a systematic method, just the modeling of one leg will be addressed here. For modeling of the three others limbs, ones just have to repeat the procedure with the parameters of each limb.

3.2.1 Screw-based Modeling of One Leg

The topology of a kinematic chain that represents an humanoid leg can be of different types, depending on the kind of movements that is expected from the chain. In the case of this paper, the chain of the considered leg has six actuated joint and three links. The distribution of the joints on the kinematic chain and its links can be seen in Fig. 3.

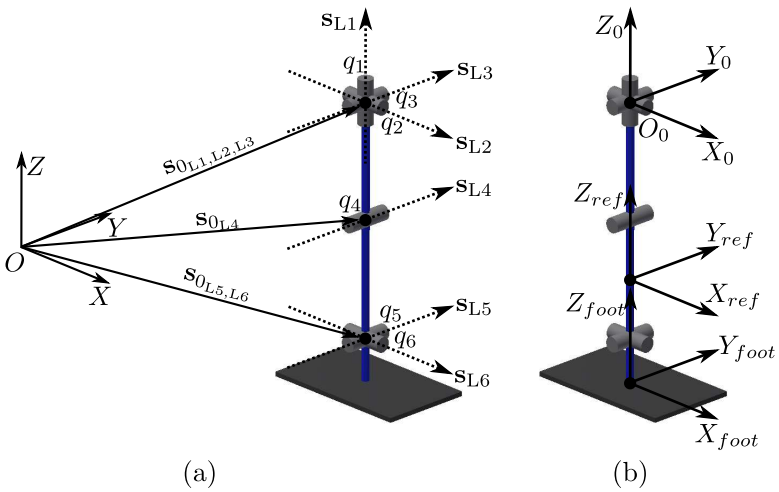

Figure 3: Kinematic chain that represents one leg: (a) identification of the screw parameters; (b) three reference frames allocated in the leg.

Once the screw parameters are identified in Fig. 3a, the screw of each joint can be determined like Eq. (4):

$$\$_{\mathbf{L_i}} = \hat{\$}_{\mathbf{L_i}} \dot{q}_{L_i}, \tag{12}$$

in which L_i is the joint i of the leg and $\dot{q}_{L_i}$ is the magnitude of the angular velocity of the joint i. All the screws of the leg can be determined using the data in Tab. 1 and Tab. 3.

Equation (5) is the Jacobian matrix of a kinematic chain representing one leg, illustrated by Fig. 3, is

$$\mathbf{J_L} = \begin{bmatrix} \hat{\$}_{\mathbf{L_1}} & \hat{\$}_{\mathbf{L_2}} & \hat{\$}_{\mathbf{L_3}} & \hat{\$}_{\mathbf{L_4}} & \hat{\$}_{\mathbf{L_5}} & \hat{\$}_{\mathbf{L_6}} \end{bmatrix}.$$

As $\mathbf{J_L}$ is a square matrix, it can be inverted to compute the inverse differential kinematic of this chain.

Direct Kinematics of One Leg

The position and orientation of the end-effector of a serial kinematic chain can be determined using Eq. (3). In Fig. 3b, the thigh, calf and foot links are labeled as L_{L1}, L_{L2} and L_{L3}, respectively. The base frame (frame 0) is allocated in the intersection point between the screw axis of the joints q_1, q_2 and q_3. The end-effector frame, called here as $foot$ frame, is allocated in a point collinear to the link L_{L3} on the sole of the foot.

Table 3: Screw parameters of the leg shown in Fig. 3a.

Joint	s	s_0	**Magnitude**
1	$\begin{bmatrix} 0 & 0 & 1 \end{bmatrix}^T$	$\begin{bmatrix} s_{0_{L1x}} & s_{0_{L1y}} & s_{0_{L1z}} \end{bmatrix}^T$	$\dot{q}_{L1}$
2	$\begin{bmatrix} 1 & 0 & 0 \end{bmatrix}^T$	$\begin{bmatrix} s_{0_{L2x}} & s_{0_{L2y}} & s_{0_{L2z}} \end{bmatrix}^T$	$\dot{q}_{L2}$
3	$\begin{bmatrix} 0 & 1 & 0 \end{bmatrix}^T$	$\begin{bmatrix} s_{0_{L3x}} & s_{0_{L3y}} & s_{0_{L3z}} \end{bmatrix}^T$	$\dot{q}_{L3}$
4	$\begin{bmatrix} 0 & 1 & 0 \end{bmatrix}^T$	$\begin{bmatrix} s_{0_{L4x}} & s_{0_{L3y}} & s_{0_{L4z}} \end{bmatrix}^T$	$\dot{q}_{L4}$
5	$\begin{bmatrix} 0 & 1 & 0 \end{bmatrix}^T$	$\begin{bmatrix} s_{0_{L5x}} & s_{0_{L5y}} & s_{0_{L5z}} \end{bmatrix}^T$	$\dot{q}_{L5}$
6	$\begin{bmatrix} 1 & 0 & 0 \end{bmatrix}^T$	$\begin{bmatrix} s_{0_{L6x}} & s_{0_{L6y}} & s_{0_{L6z}} \end{bmatrix}^T$	$\dot{q}_{L6}$

It is necessary to allocate another reference frame that will be used to determine the matrix $\bar{\mathbf{A}}^{\mathbf{c}}_{\mathbf{r}}$ and $\bar{\mathbf{A}}^{\mathbf{r}}_{\mathbf{k}}$ of Eq. (3). Allocating the reference frame (called ref) in the middle of link L_{L2} (Fig. 3b), the vectors $\mathbf{s_{0_{Li}}}$ are determined with the new reference as:

$$\mathbf{s_{0_{L1}}} = \mathbf{s_{0_{L2}}} = \mathbf{s_{0_{L3}}} = \begin{bmatrix} 0 \\ 0 \\ L_{L1} + \frac{L_{L2}}{2} \end{bmatrix}, \ \mathbf{s_{0_{L4}}} = \begin{bmatrix} 0 \\ 0 \\ \frac{L_{L2}}{2} \end{bmatrix} \text{ and } \mathbf{s_{0_{L5}}} = \mathbf{s_{0_{L6}}} = \begin{bmatrix} 0 \\ 0 \\ -\frac{L_{L2}}{2} \end{bmatrix}. \tag{13}$$

The $\bar{\mathbf{A}}^{\mathbf{0}}_{\mathbf{ref}} = \bar{\mathbf{A}}^{\mathbf{c}}_{\mathbf{r}}$ and $\bar{\mathbf{A}}^{\mathbf{ref}}_{\mathbf{foot}} = \bar{\mathbf{A}}^{\mathbf{r}}_{\mathbf{k}}$ are, respectively, the position and orientation of the frame ref with respect to the base frame and the position and orientation of the frame $foot$ with respect to the frame ref:

$$\bar{\mathbf{A}}^{\mathbf{0}}_{\mathbf{ref}} = \begin{bmatrix} 1 & 0 & 0 & 0 \\ 0 & 1 & 0 & 0 \\ 0 & 0 & 1 & -\left(L_{L1} + \frac{L_{L2}}{2}\right) \\ 0 & 0 & 0 & 1 \end{bmatrix}; \quad \bar{\mathbf{A}}^{\mathbf{ref}}_{\mathbf{foot}} = \begin{bmatrix} 1 & 0 & 0 & 0 \\ 0 & 1 & 0 & 0 \\ 0 & 0 & 1 & -\left(\frac{L_{L2}}{2} + L_{L3}\right) \\ 0 & 0 & 0 & 1 \end{bmatrix}. \tag{14}$$

The matrices $\mathbf{A}^{\mathbf{ref}}_{\mathbf{q_{Li}}}$ are the matrices formed by the screw of each joint of the leg in respect to the frame ref (Fig. 3) using Rodrigues's formula as in Tsai (1999).

3.2.2 Differential Kinematics of the Whole Humanoid Body

On the earlier sections, it was demonstrated, separately, how the ST can be used to model the kinematics of a chain that represents an humanoid leg. After modeling the three others limbs, it is necessary to represent all four chains at the same reference frame on the humanoid structure to have a full-body kinematic model of an HR.

The waist is the local reference frame in the humanoid structure from which part the chains of the limbs. Therefore, a transformation must be done to represent the leg and the arm (earlier modeled in the fixed base frame) chains with respect to the waist of the humanoid. The transformation needed is made by the Eq. (6) as illustrated by the Fig. 4.

The matrix $\mathbf{T^w_{RL}}$ "transforms" a generic leg (Fig. 3) to the right leg of the humanoid and it is composed by the skew-symmetric matrix $\hat{\mathbf{p}}^{\mathbf{w}}_{\mathbf{RL}}$ and the rotation matrix $\mathbf{R^w_{RL}}$ (Eq. (6)). The same can be done about the arm, that is, the matrix $\mathbf{T^w_{RS}}$ would "transform" a generic arm to the right arm of the robot; and it would be composed by the skew-symmetric matrix $\hat{\mathbf{p}}^{\mathbf{w}}_{\mathbf{RS}}$ and the rotation matrix $\mathbf{R^w_{RS}}$. Because of the bilateral symmetry of the human body, the determination of the left leg and left arm chains is done in a similar way as done to the right ones. That is, the transformation $\mathbf{T^w_{LL}}$ would make a generic leg (Fig. 3) be the left leg and, likewise, the transformation $\mathbf{T^w_{LS}}$ would make a generic arm be the left arm.

The matrices $\mathbf{R^w_{RL}}$, $\mathbf{R^w_{RS}}$, $\mathbf{R^w_{LL}}$ and $\mathbf{R^w_{LS}}$ are 3×3 identity matrices since there is no change between the orientations of the frames (Fig. 4). However, the vectors $\mathbf{p^w_{RL}}$, $\mathbf{p^w_{RS}}$, $\mathbf{p^w_{LL}}$ and $\mathbf{p^w_{RS}}$ that compose the skew-symmetric matrices are determined by the data in Tab. 2 (see Tsai (1999) for more details).

By placing the four limbs with respect to the humanoid waist in the robot structure, the whole HR body is formed as can been seen in Fig. 2. It is composed by a FB allocated in its waist (that is, an 3P3R virtual kinematic chain attached between the considered inertial reference frame and the waist frame) and four serial kinematic chains that work together to perform a task, for example, making a gait or manipulating an object.

Using DH parameters, it would be necessary to have two kinematic representations to the same kinematic chain, depending on which foot is supporting the robot. Moreover, to solve its differential kinematics, there would be five Jacobian matrices to be considered: the first between the inertial reference frame, and the humanoid's waist and, the other four, for each limb, are with respect to the waist of the robot. Thus, to planning motion to the HR, it is necessary to consider the motion planning of the hands and the legs with respect to the waist.

However, by the use of the virtual chains, an HR structure can be represented as a closed mechanism and, then, apply the Davies's method, by the ST, to solve its differential kinematics. Here, the virtual chains are used to impose motion to the "real" kinematic chains of the biped. And, by that, the motion planning can be done in the inertial reference frame as planning motion to five collaborative robots.

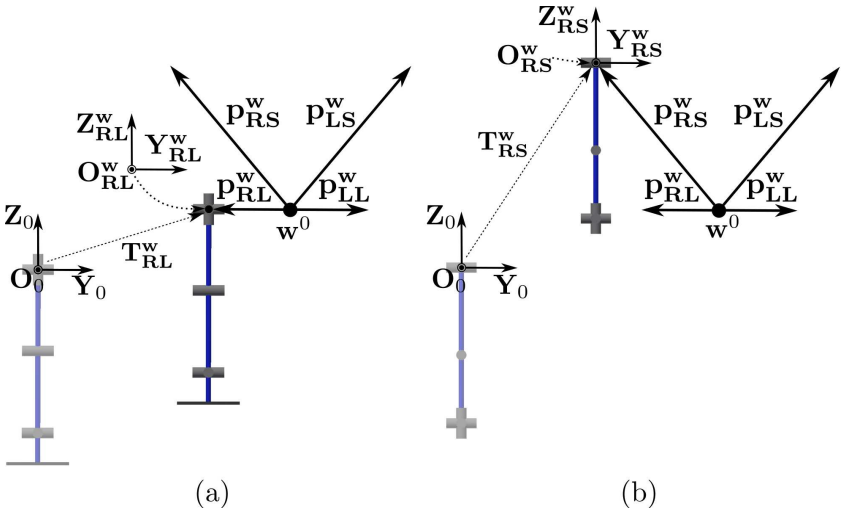

Figure 4: Frame reference transformation: (a) transformation to the right leg; (b) transformation to the right arm.

As the motion is spatial, five 3P3R virtual chains are used: one to be the FB attached to the robot's waist, and the four others are linked, each one, on the feet and on the hands. The resulting mechanism is a complex spatial parallel mechanism with four loops composed by fifty four joints and fifty one links, as it can be seen in the graph notation (Tsai, 2001; Campos *et al.*, 2005) illustrated by Fig. 5.

In Fig. 5, the arrows are the joints named as: $\$_{\mathbf{vtorsoi}}$ is the virtual joint i of the torso; $\$_{\mathbf{vji}}$ is the joint i of the virtual chain attached to the "real" chain j ($j \in \{rl \quad ll \quad ra \quad la\}$ for right leg, left leg, right arm and left arm, respectively); and $\$_{\mathbf{ji}}$ is the joint i of the "real" chain j. Moreover, the vertices are the links of the mechanism and they are designated as: $VLTi$ is the virtual link i of the virtual chain attached to the waist; $VLji$ is the virtual link i of the virtual chain j; ji is the link i of the "real" chain j ($j \in \{RL \quad LL \quad RA \quad LA\}$ for right leg, left leg, right arm and left arm, respectively); Torso, RF, LF, RHand, LHand and Floor are, respectively, the links of the waist, right foot, left foot, right "hand", left "hand", and the ground (where the biped walks on).

Now, with the HR represented as a closed mechanism composed by four loops, it is possible to apply the Davies's method to solve the differential kinematics for the whole body at once. First, the network matrix $\mathbf{N}$ has to be assembled with the normalized screws. As the mechanism has fifty four joints and four loops, therefore, the matrix $\mathbf{N}$ has dimension 24×54, and the magnitude vector has dimension 24×1.

Calculating the mobility of the parallel mechanism illustrated in Fig 5, the result is thirty: twenty four real joints plus the six DoF of the FB. That is, the mobility of the humanoid structure was not changed by the inclusion of the virtual chains, therefore, the Kirchhoff-Davies law can by applied without any problem or consideration.

As the method states, it is necessary to identify and to distinguish the primary and the secondary joint variables in the magnitude vector. As this work uses the virtual chains to impose motion to the "real" chain, then, the joints of the virtual chains were chosen to be the primary velocities. That means,

$$\dot{\mathbf{q}} = \begin{bmatrix} \dot{\mathbf{q}}_\mathbf{s}^\mathbf{T} & \dot{\mathbf{q}}_\mathbf{p}^\mathbf{T} \end{bmatrix}^T, \tag{15}$$

in which $\dot{\mathbf{q}}_\mathbf{s}$ is formed by the first twenty four lines of the vector $\dot{\mathbf{q}}$ ("real" joint velocities) and $\dot{\mathbf{q}}_\mathbf{p}$ is assembled by the last thirty lines (virtual joint velocities). Choosing $\mathbf{N_p}$ and $\mathbf{N_s}$ coherently with $\dot{\mathbf{q}}_\mathbf{s}$ and $\dot{\mathbf{q}}_\mathbf{p}$, respectively, the Davies's method can be applied as it states in Eq. (9), and differential kinematics of the whole body is solved.

4. TRAJECTORY GENERATION

Biped anthropomorphic robots are composed by three or more serial kinematic chains that are detached from an inertial reference frame and its configuration varies in time. Therefore, it is not only necessary that the biped motion ensures the structural stability of the robot, but also it has to guarantee that the robot will not fall down on the ground during its motion.

The generation of the trajectory is made using the geometric constraint method in a similar way as done in (Huang *et al.*, 2001; Wang *et al.*, 2009), because, besides being intuitive, to apply this method, it is not necessary to use the switching models by using FB, the ST and its tool.

Firstly, it is needed to choose points on the humanoid structure for which the trajectory will be generated. As it was said before and because of the use of the virtual chains, these points are the ones in which were attached the virtual chains on the humanoid: its waist, feet and hands. Then, for each point of interest, one trajectory is elaborated using third order spline interpolation (Huang *et al.*, 2001). As global parameters: the number of steps k; T_c is its period in seconds; and j is a counter. The notation used here is: K_{ij} in which $K \in \{X \quad Y \quad Z\}$ indicates the axis of the motion; $i \in \{R \quad L\}$ for right and left; and $j \in \{F \quad A\}$ for foot and arm.

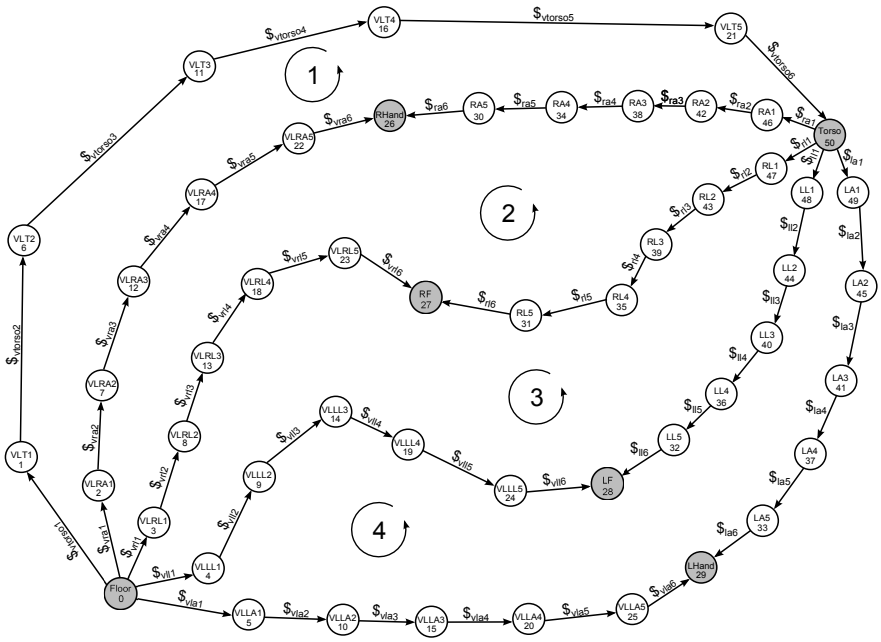

Figure 5: Graph representation of the parallel mechanism composed by the humanoid and virtual chains with the designation of the number of circuits and its directions.

4.1 Trajectory Generation for the Arms

During a gait, the arms have a passive role - they are not used to manipulate objects or tools and they do not rely on any point in space - because they are used to assist on structural balance of the biped mechanism. Thus, their trajectory was generated considering only the swing motion as in a humanoid gait.

Considering the maximum displacement $X_{max} = 0,03\ m$ and the minimum $X_{min} = 0$ both with respect to the X axis, considering also the maximum displacement $Z_{max} = 0,0187\ m$ and the minimum $Z_{min} = 0$ both with respect to the Z axis, and g ($g \in \{ -1, \quad 1 \}$), the trajectories of the arms with respect to the X and Z axis are determined by the equations Eq. (16), Eq. (17), and Eq. (18).

$$X_{RA}(t) = \begin{cases} gX_{max}, & jT_c \le t < (j+0,1)\,T_c \\ gX_{min}, & t = (j+0,5)\,T_c \\ -gX_{max}, & (j+0.89)\,T_c < t \le (j+1)\,T_c \end{cases} \tag{16}$$

$$X_{LA}(t) = \begin{cases} -gX_{max}, & jT_c \le t < (j+0.1)\,T_c \\ gX_{min}, & t = (j+0,5)\,T_c \\ gX_{max}, & (j+0.89)\,T_c < t \le (j+1)\,T_c \end{cases} \tag{17}$$

$$Z_A(t) = \begin{cases} Z_{max}, & jT_c \le t < (j+0,1)\,T_c \\ Z_{min}, & t = (j+0,5)\,T_c \\ Z_{max}, & (j+0.89)\,T_c < t \le (j+1)\,T_c \end{cases}, \tag{18}$$

4.2 Trajectory Generation for the Foot

In the initial position of the HR, the left foot is forward of the right one by a distance of $Step_{ini} = 0,1\ m$. The step length is $Step = 0,2\ m$ and its maximum high during one step is $Z_{max} = 0,03\ m$ ($Z_{min} = 0$). In the gait planning, it was considered that the robot remains on the double support phase (when the biped is supported by both feet) to reallocate the ground projection of the center of mass (GCoM) from the previous support to under the next support foot.

As the feet are composed by just one piece, then, it is not necessary to change the orientation of the feet during the gait. That is, in a human gait, as the foot has one DoF, it gets off the ground in two movements: the first one boosts forward the body in the direction of the gait, and the second finishes the double support phase. As the humanoid illustrated by Fig. 2 has one piece foot, thus, the feet get off the ground in just one movement. The trajectories of the feet with respect to the

X and Z axis are determined by the equations Eq. (19), Eq. (20), Eq. (21), and Eq. (22). Graphically, the trajectories of the feet with respect to de X and Z axis can be seen in Fig. 6 and Fig. 7.

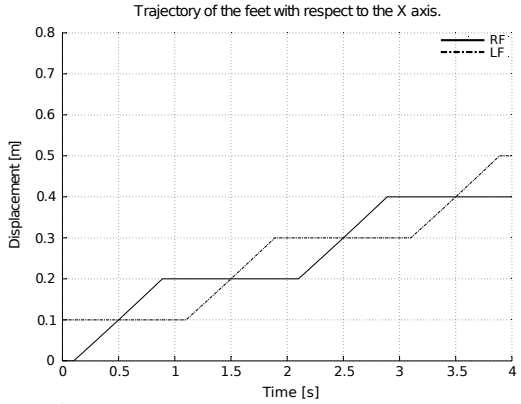

Figure 6: Trajectories of the feet with respect to the X axis.

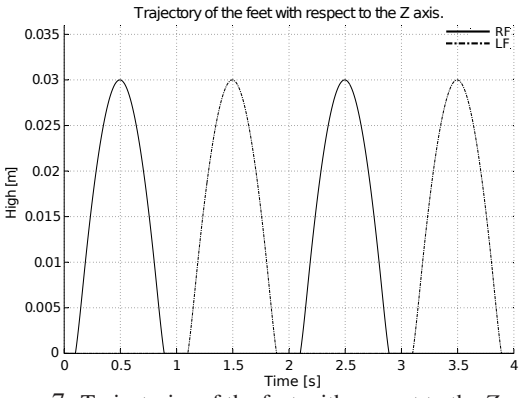

Figure 7: Trajectories of the feet with respect to the Z axis.

$$X_{RF}(t) = \begin{cases} jStep, & 0 \le t < (j+0.1)\,T_c \\ (j+0,5)\,Step, & t = (j+0,5)\,T_c \\ (j+1)\,Step, & (j+0,89)\,T_c \le t < (j+2)\,T_c \end{cases} \tag{19}$$

$$X_{LF}(t) = \begin{cases} Step_{ini} + jStep, & 0 \le t < (j+1)\,T_c \\ Step_{ini} + (j-1)\,Step, & (j+1)\,T_c \le t < (j+1,01)\,T_c \\ Step_{ini} + (j-0,5)\,Step, & t = (j+1,5)\,T_c \\ Step_{ini} + jStep, & (j+1,89)\,T_c \le t < (j+2)\,T_c \end{cases} \tag{20}$$

$$Z_{RF}(t) = \begin{cases} Z_{min}, & 0 \le t < (j+0,1)\,T_c \\ 0,1Z_{max}, & t = (j+0,1)\,T_c + 0,03 \\ 0,3Z_{max}, & t = (j+0,1)\,T_c + 0,08 \\ Z_{max}, & t = (j+0,5)\,T_c \\ 0,3Z_{max}, & t = (j+0,89)\,T_c - 0,08 \\ 0,1Z_{max}, & t = (j+0,89)\,T_c - 0,03 \\ Z_{min}, & (j+0,89)\,T_c \le t < (j+2)\,T_c \end{cases} \tag{21}$$

$$Z_{LF}(t) = \begin{cases} Z_{min}, & 0 \le t \le (j+1,1)\,T_c \\ 0,1Z_{max}, & t = (j+1,1)\,T_c + 0.03 \\ 0,3Z_{max}, & t = (j+1,1)\,T_c + 0.08 \\ Z_{max}, & t = (j+1,5)\,T_c \\ 0,3Z_{max}, & t = (j+1,89)\,T_c - 0.08 \\ 0,1Z_{max}, & t = (j+1,89)\,T_c - 0.03 \\ Z_{min}, & (j+1,89)\,T_c \le t < (j+2)\,T_c \end{cases} \tag{22}$$

4.3 Trajectory Generation for the Hip/Waist

For the generate of the trajectory of the waist, firstly the trajectory in the Z axis would be done "arbitrarily" because the movement with respect to Z axis of the center of mass does not affect expressively the location of the ZMP (Huang *et al.*, 2001). However, the position of the waist with respect to the Z axis remains the same for all motions as it was done in the 3D-LIP approach (Kajita *et al.*, 2001).

Given the proximity of the center of mass and the waist, these two points will be treated as equals. Therefore, the trajectory generation to the waist with respect to the X and Y axis, respectively, are generated in a way that the motion of the center of mass ensures a balanced gait by the ZMP criterion (Kajita *et al.*, 2003). That is, as it is considered a quasi-static motion, if the GCoM always remains inside of the support polygon, the humanoid will not fall down. Moreover, the proximity between the GCoM and the ZMP ensures a balanced gait.

Thus, considering the initial position of the hip with respect to the X axis as $X_{HIP_{ini}} = 0,05\ m$, the variation of the displacement with respect to the X axis as $\Delta X_{HIP} = 0,025\ m$, that in $t = 0\ X_{HIP}(0) = X_{HIP_{ini}}$ and assuming $X_{HIP}(t_i) \equiv X_{HIP}(i)$, the trajectory of the hip/waist with respect to the X axis is given by:

$$X_{HIP}(i) = \begin{cases} X_{HIP}(i-1), & t = jT_c \\ X_{HIP}(i-1) + \Delta X_{HIP}, & t = (j+0,1)\,T_c \\ X_{HIP}(i-1) + \Delta X_{HIP}, & t = (j+0,9)\,T_c \\ X_{HIP}(i-1) + \Delta X_{HIP}, & t = (j+1)\,T_c. \end{cases} \tag{23}$$

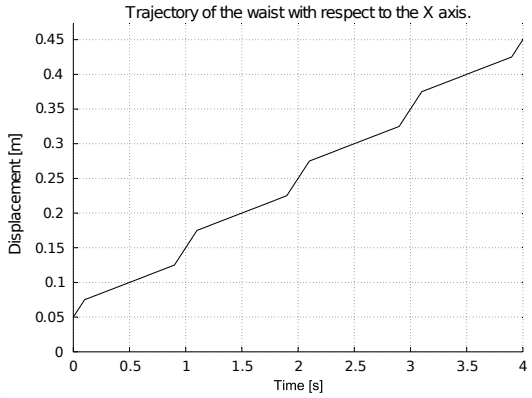

Figure 8: Trajectory of the waist with respect to the X axis.

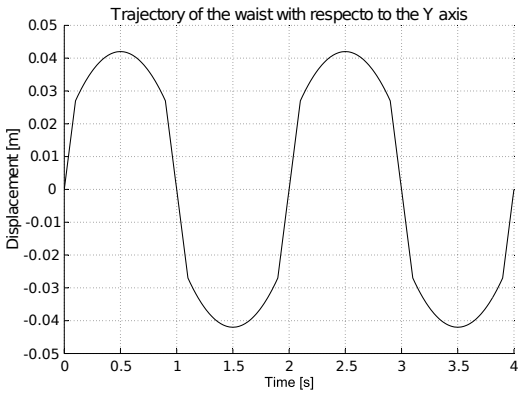

Figure 9: Trajectory of the waist with respect to the Y axis.

Now, considering three displacements quantities, $Y_{HIP_1} = 0\ m$, $Y_{HIP_2} = 0,027\ m$ and $Y_{HIP_3} = 0,042\ m$ and that s can assume two values: -1 if the supporting foot is the right one, and -1 if it is the left one, then, the trajectory of the hip/waist with respect to the Y axis is given by:

$$Y_{HIP}(t) = \begin{cases} Y_{HIP_1}, & t = jT_c \\ sY_{HIP_2}, & t = (j+0,1)\,T_c \\ sY_{HIP_3}, & t = (j+0,5)\,T_c \\ sY_{HIP_2}, & t = (j+0,9)\,T_c \\ Y_{HIP_1}, & t = (j+1)\,T_c. \end{cases} \tag{24}$$

Graphically, both trajectories can be seen in Fig. 8 and Fig. 9.

5. RESULTS

In the previous section, the trajectory generation used in this work was presented. In Fig. 10, it can be seen the HR in four different instants, during the execution of the trajectory. Actually, in the same figure, the robot is shown in the beginning/ending of each gait cycle.

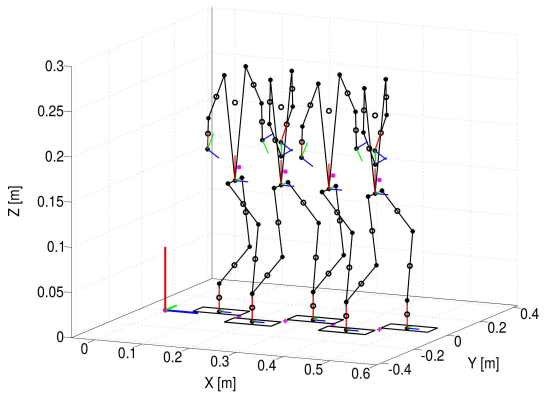

Figure 10: Video frames of the humanoid while walking.

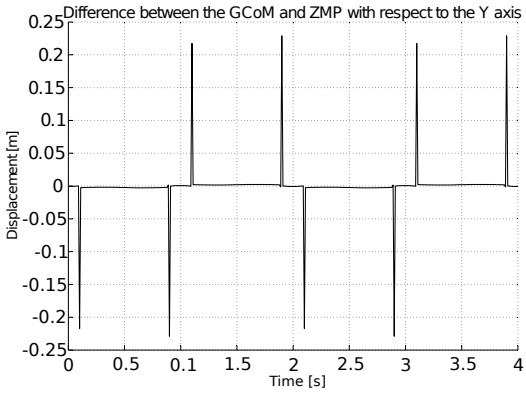

Figure 11: Difference between the GCoM and ZMP with respect to the Y axis.

After determining the equations that characterize the trajectories, it was used a third order interpolation spline to generate smooth curves. Even so, it can be seen in Fig. 13 some discontinuity with respect to the angular displacement of the joints. That is because the position of the joints are calculated by the inverse kinematic and it was made analytically.

It can be seen in Fig. 11 and Fig. 12 the difference of position between the GCoM and the ZMP. In the same figures, ones may see that almost all time, the ZMP keeps a distance from the GCoM that ensures the ZMP inside of the supporting polygon. In Fig. 11 and Fig. 12, it also can be seen that there are spikes that make the ZMP move away from the GCoM. But given geometry of the feet and the short time in that it occurs, it can be said that, despite of those spikes, the trajectory generated is balanced by the ZMP criterion and the robot will not fall down.

By the simulation, some discontinuities were found on the joints velocities profiles that would explain the existence of the spikes seen. Smooth those discontinuities would be one of the ways that one could achieve a reduction of the peaks

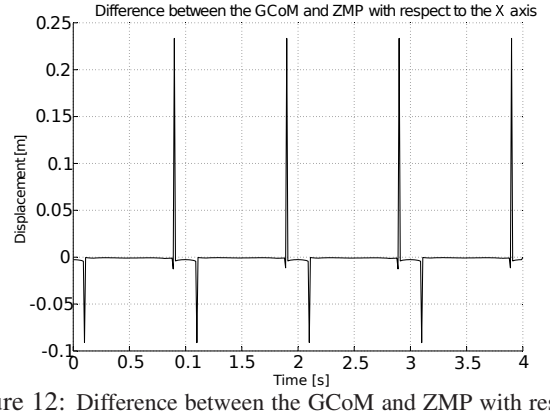

Figure 12: Difference between the GCoM and ZMP with respect to the X axis.

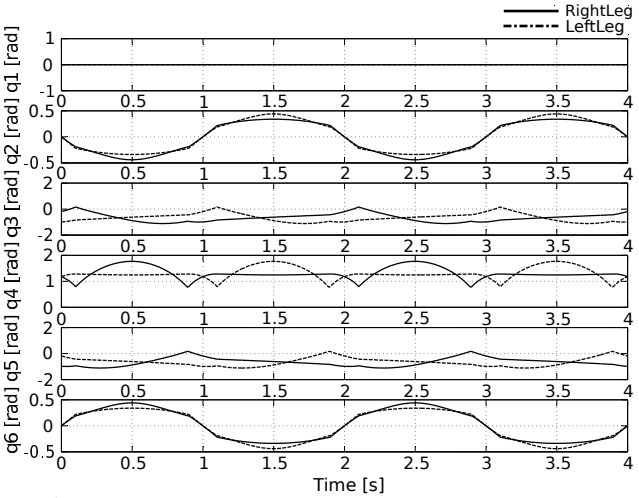

Figure 13: Angular displacement of the joints os the legs.

observed in Fig. 12 and Fig. 11. The trajectory can be improved, that is, to decrease the spikes, by choosing a better initial and final velocities. The method utilized in this work generates the trajectory with respect of the position in the workspace of each virtual chain and, then, the velocity is calculated by numerical methods.

6. CONCLUSION

This paper presented in a systematic way how to use the floating base concept, screw theory and its tools to model a full-body humanoid robot. With the floating base concept, the humanoid robot could be modeled in such a way that it has only one kinematic model independent of the supporting leg. Moreover, by the use of the virtual chains, it was possible to represent a humanoid chain as a closed mechanism and, then, apply Davies's method to solve the inverse differential kinematics of the whole body at once.

This work also showed that the virtual chains can be used to impose motion to "real" chains. By the use of virtual chains, the whole trajectory was elaborated in the inertial reference frame. To generate trajectory for humanoid robots using virtual chains is almost like to generate trajectories for a multi-robot system since the virtual chains can be understood as five different serial robots working together to perform a gait. This approach allows to use various methods and tools of the collaborative robotics in humanoid robots.

The gait generator presented in this work used the geometric constraint method because, besides being intuitive, to apply this method, it is not necessary to use the switching models since the floating base concept, the screw theory and its tool are used. The generator is composed by some parameters and to generate different kinds of gaits or motion, only some of this parameters need to be changed.

To validate and to check the feasibility of the gait generated, it was used the ZMP criterion. The generator proposed in this work is capable to create balanced gait without making the humanoid robot fall down to the ground. Considering the geometry of the feet and the very short time in which the spikes occur, this work let to conclude that, despite the spikes, the generated gait is balanced.

For future works, there will be a continuous study in how the tools of the screw theory may contribute to humanoid robotics field. It would be very interesting and promising to analyze the biped robot including the static and dynamic models of the humanoid robot also by the screw theory.

7. ACKNOWLEDGEMENTS

The authors thank the UFSC, CNPq and CAPES for the infrastructure and funding granted.

8. REFERENCES

Bottema, O.O. and Roth, B., 1979. *Theoretical Kinematics*. North-Holand Pub. Co., New York.

Campos, A., Guenther, R. and Martins, D., 2005. "Differential kinematics of serial manipulators using virtual chains". *J. of the Braz. Soc. of Mech. Sciences and Engineering (ABCM)*, Vol. 27, pp. 345–356.

Davidson, J.K. and Hunt, K.H., 2004. *Robots and screw theory: applications of kinematics and statics to robotics*. Oxford University Press on Demand.

Davies, T.H., 1981. "Kirchhoff's circulation law applied to multi-loop kinematic chains". *J. of Mechanism and Machine Theory*, Vol. 16, No. 3, pp. 171–183.

Denavit, J., 1955. "A kinematic notation for lower-pair mechanisms based on matrices". *Trans. of the ASME - J. of Applied Mechanics*, Vol. 22, pp. 215–221.

Gal, J.A., Gallo, L.M., Palla, S., Murray, G. and Klineberg, I., 2004. "Analysis of human mandibular mechanics based on screw theory and in vivo data". *J. of Biomechanics*, Vol. 37, No. 9, pp. 1405–1412.

Guenther, R., Simas, H., da Cruz, D. and Martins, D., 2008. *A new integration method for differential inverse kinematics of closed-chain robots*, ABCM, RJ/Brazil, Vol. 3, pp. 225–235.

Hoonsuwan, P., Sillapaphiromsuk, S., Sukvichai, K. and Fish, A., 2009. "Designing a stable humanoid robot trajectory using a real human motion". In *6th Inter. Conf. on Elect. Engineering/Electronics, Computer, Telecom. and Information Tech. (ECTI-CON)*. IEEE, Vol. 1, pp. 336–339.

Huang, Q., Yokoi, K., Kajita, S., Kaneko, K., Arai, H., Koyachi, N. and Tanie, K., 2001. "Planning walking patterns for a biped robot". *IEEE Trans. on Robotics and Automation*, Vol. 17, No. 3, pp. 280–289.

Hugel, V. and Jouandeau, N., 2012. "Walking patterns for real time path planning simulation of humanoids". In *RO-MAN*. IEEE, pp. 424–430.

Hunt, K.H., 2000. "Don't cross-thread the screw". In *A Symposium Commemorating The Legacy, Works and Life of Sir Robert Stawell Ball Upon the 100th Anniversary of A Treatise on The Theory of Screws*. University of Cambridge, Trinity College, Cambridge University Press, Cambridge, pp. 1–37.

Kajita, S., Kanehiro, F., Kaneko, K., Fujiwara, K., Harada, K., Yokoi, K. and Hirukawa, H., 2003. "Biped walking pattern generation by using preview control of zero-moment point". In *Proc. of the Inter. Conf. on Robotics and Automation (ICRA)*. IEEE, Vol. 2, pp. 1620–1626.

Kajita, S., Kanehiro, F., Kaneko, K., Yokoi, K. and Hirukawa, H., 2001. "The 3D linear inverted pendulum mode: a simple modeling for a biped walking pattern generation". In *Proc. of the IEEE/RSJ Inter. Conf. on Intelligent Robots and Systems (IROS)*. Vol. 1, pp. 239–246.

Man, C.H., Fan, X., Li, C.R. and Zhao, Z.H., 2007. "Kinematics analysis based on screw theory of a humanoid robot". *J. of China University of Mining and Technology*, Vol. 17, No. 1, pp. 49–52.

Mistry, M., Nakanishi, J., Cheng, G. and Schaal, S., 2008. "Inverse kinematics with floating base and constraints for full body humanoid robot control". In *8th IEEE-RAS Inter. Conf. on Humanoid Robots (Humanoids)*. pp. 22–27.

Moro, F.L., Tsagarakis, N.G. and Caldwell, D.G., 2011. "A human-like walking for the COmpliant humanoid COMAN based on CoM trajectory reconstruction from kinematic motion primitives". In *11th IEEE-RAS Inter. Conf. on Humanoid Robots (Humanoids)*. pp. 364–370.

Moro, F.L., Tsagarakis, N.G. and Caldwell, D.G., 2012. "Efficient human-like walking for the compliant humanoid COMAN based on kinematic motion primitives (KMPs)". In *Inter. Conf. on Robotics and Automation (ICRA)*. IEEE, pp. 2007–2014.

Mu, X. and Wu, Q., 2004. "Dynamic modeling and sliding mode control of a five-link biped during the double support phase". In *Proc. of the American Control Conference (ACC)*. AACC, Vol. 3, pp. 2609–2614.

Papadopoulos, E. and Dubowsky, S., 1991. "On the nature of control algorithms for free-floating space manipulators". *IEEE Trans. on Robotics and Automation*, Vol. 7, No. 6, pp. 750–758.

Ribeiro, L. and Martins, D., 2010. "Screw-based relative Jacobian for manipulators cooperating in a task using Assur's virtual chains". In *Symposium Series in Mechatronics*. ACBM, RJ/Brazil, Vol. 4, pp. 729–738.

Rocha, C.R., Tonetto, C.P. and Dias, A., 2011. "A framework for kinematic modeling of cooperative robot systems based on screw theory". In *Proc. of the 21th Inter. Congress of Mechanical Engineering (COBEM)*. ABCM, Vol. 5, pp. 1150–1159.

Sabater, J.M., Garcia, N., Perez, C., Azorin, J.M., Saltaren, R.J. and Yime, E., 2006. "Design and analysis of a spherical humanoid neck using screw theory". In *1st IEEE/RAS-EMBS Inter. Conf. on Biomedical Robotics and Biomechatronics (BioRob)*. pp. 1166–1171.

Sánchez, M.E.H., Leyva, F.J.K.L., Limón, R.C. and Zannatha, J.M.I., 2011. "Mechanical design and kinematic analysis of the AH1N1 humanoid robot". In *21st Inter. Conf. on Electrical Communications and Computers (CONIELECOMP)*. IEEE, pp. 177–183.

Santos, C., Guenther, R., Martins, D. and De Pieri, E., 2006. "Virtual kinematic chains to solve the underwater vehicle-manipulator systems redundancy". In *J. of the Braz. Soc. of Mech. Sciences and Engineering*. ABCM, Vol. 28, pp. 354–361.

Sentis, L., 2007. *Synthesis and control of whole-body behaviors in humanoid systems*. Ph.D. thesis, Stanford, CA, USA.

Simas, H., 2008. *Planejamento de trajetórias e evitamento de colisão em tarefas de manipuladores reduntantes operando em ambientes confinados*. Ph.D. thesis, Universidade Federal de Santa Catarina, Centro Tecnológico. Programa de Pós-graduação em Engenharia Mecânica, Florianópolis, Santa Catarina, Brasil.

Toscano, G.S., Simas, H. and Castelan, E.B., 2011. "Modelagem de um gerador de trajetória retilínea no espaço cartesiano para robô antropomórfico espacial". *X Simpósio Brasileiro em Automação Inteligente (SBAI)*, Vol. 10, pp. 683–688.

Tsai, L.W., 1999. *Robot analysis: the mechanics of serial and parallel manipulators*. Wiley-Interscience, New York.

Tsai, L.W., 2001. *Mechanism design: enumeration of kinematic structures according to function*, Vol. 16. CRC press.

Wang, F., Zhu, W. and Na, L., 2009. "Gait planning and simulation of Robonova-1 robot". In *2nd Inter. Conf. on Intelligent Computation Technology and Automation (ICICTA)*. Vol. 3, pp. 411–414.

Westervelt, E.R., Grizzle, J.W., Chevallereau, C., Choi, J.H. and Morris, B., 2007. *Feedback control of dynamic bipedal robot locomotion*. CRC press, Boca Raton.

Zhu, D., Zhu, J. and Fang, Y., 2009. "Analysis of a novel parallel manipulator for rotary humanoid Wrist based on screw theory". In *IEEE Inter. Conf. on Robotics and Biomimetics (ROBIO)*. pp. 983–987.

9. RESPONSIBILITY NOTICE

The authors are the only responsible for the printed material included in this paper.